

Supporting Information for “Photoluminescence Redshift of AgInS₂ Quantum Dots by Employing Shells with Graded Composition”

Navapat KROBKONG,^a Taro UEMATSU,^{a,b,*,§} Tsukasa TORIMOTO,^{c,§§} and Susumu KUWABATA,^{a,b,*,§§}

^a *Department of Applied Chemistry, Graduate School of Engineering, Osaka University, 2-1 Yamada-oka, Suita, Osaka 565-0871, Japan*

^b *Innovative Catalysis Science Division, Institute for Open and Transdisciplinary Research Initiatives (ICS-OTRI), Osaka University, 2-1 Yamada-oka, Suita, Osaka 565-0871, Japan*

^c *Department of Materials Chemistry, Graduate School of Engineering, Nagoya University, Furo-cho, Chikusa-ku, Nagoya, Aichi 464-8601, Japan*

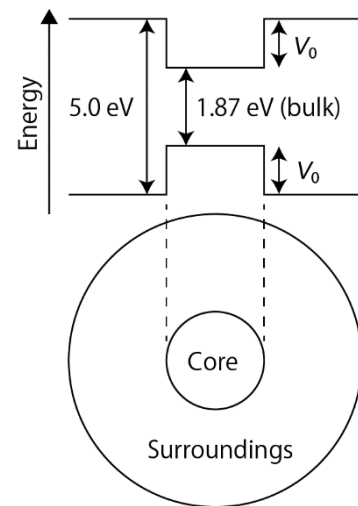
*Corresponding Authors: t-uematsu@chem.eng.osaka-u.ac.jp, (T. U.),
kuwabata@chem.eng.osaka-u.ac.jp (S. K.)

Sample preparation and calibration standard of an inductively coupled plasma atomic emission spectroscopy (ICP–AES).

A 50 μL of purified QD solution was dried and digested with concentrated nitric acid at 110 $^{\circ}\text{C}$ for 4 h. During cooling, a 0.5 mL of H_2O_2 was added and the reaction was continued for another 1 h. The samples were then diluted to a fixed ratio with 0.1 M HNO_3 . An ICP–AES setup equipped with a sequential spectrometer (Shimadzu, ICPS-7510) was used. To determine the concentration of the elements, the atomic emission intensity was compared with a calibration curve, which was prepared each time before measuring unknown samples. The intensity was measured by integrating for 1 min at the wavelength where no overlap with other elements was previously confirmed.

Effective mass approximation

To verify that the observed peak shifts are reasonable, we predicted the bandgap change due to quantum size effects using the finite depth effective mass approximation (FDEMA). This model is suitable for predicting quantum size effects observed in regions with relatively large particle sizes. The parameters used include the bulk bandgap of nanoparticle materials (E_g), the electron mass (m_e), the hole mass (m_h), the energy difference between the core and matrix (ligand) (V_0), and the relative permittivity (ϵ_r) of the semiconductor. A unique feature of this method is that it considers the leakage of the wave function into the matrix, which does not exist when infinitely high walls are assumed.



The Schrödinger equation in spherical coordinates is

$$-\frac{\hbar^2}{2m} \left(\frac{\partial^2}{\partial r^2} + \frac{2}{r} \frac{\partial}{\partial r} + \frac{1}{r^2} \nabla^2 \right) \psi(r, \theta, \phi) + V\psi(r, \theta, \phi) = E\psi(r, \theta, \phi) \quad (1)$$

where \hbar and ψ are Planck's constant divided by 2π and the eigenfunction, respectively, and E is the energy eigenvalue of the particle of mass m . When angular momentum quantum number, l , is equal to 0, the equation can be simplified as

$$-\frac{\hbar^2}{2m} \left(\frac{d^2}{dr^2} + \frac{2}{r} \frac{d}{dr} \right) R(r) + VR(r) = ER(r) \quad (2)$$

with the eigenfunction $R(r)$ separated from $\psi(r, \theta, \phi)$ to have only the radial function. In the case of the spherical particle, the potential V of the above equation is centrosymmetric and can be described as

$$V(r) = \begin{cases} 0, & r < r_0 \\ V, & r > r_0 \end{cases} \quad (3)$$

using the radial distance r and the particle radius r_0 . Therefore, eq 2 can be rewritten as

$$\frac{d^2 R(r)}{dr^2} + \frac{2}{r} \frac{dR(r)}{dr} + \left(\frac{2mE}{\hbar^2} \right) R(r) = 0 \quad (r < r_0, \text{core}) \quad (4)$$

$$\frac{d^2 R(r)}{dr^2} + \frac{2}{r} \frac{dR(r)}{dr} - \left(\frac{2m|E - V_0|}{\hbar^2} \right) R(r) = 0 \quad (r > r_0, \text{surroundings}) \quad (5)$$

where V_0 is the potential gap between the core and the surroundings. The following substitutions

$$k_{\text{in}}^2 = \frac{2mE}{\hbar^2} \quad (6)$$

$$k_{\text{out}}^2 = \frac{2m|E - V_0|}{\hbar^2} \quad (7)$$

gives the following eigenfunctions:

$$R(r) \propto \frac{\sin(k_{\text{in}} r)}{k_{\text{in}} r} \quad (\text{Bessel function}) \quad (8)$$

$$R(r) \propto -\frac{\exp(k_{\text{out}} r)}{k_{\text{out}} r} \quad (\text{Hankel function}) \quad (9)$$

Applying a boundary condition

$$\frac{\sin(k_{\text{in}} r_0)}{k_{\text{in}} r_0} = -\frac{\exp(k_{\text{out}} r_0)}{k_{\text{out}} r_0} \quad (10)$$

gives the energy eigenvalue defined in eq 6, and the eigenvalues for the electron in the conduction band and the hole in the valence band become the energy offsets from the bulk state (ΔE_e and ΔE_h).

On the other hand, there is a Coulomb interaction between the electron and the hole. This can be calculated with a simple equation

$$E_{\text{coul}} = -1.75 \times \frac{e^2}{\epsilon R} \quad (11)$$

using the relative permittivity, ϵ , and the elementary charge, e .

Taking all factors together, the bandgap variation due to particle size is

$$E_g = \Delta E_e + \Delta E_h + E_{\text{coul}} + E_{g, \text{bulk}} \quad (12)$$

The parameters used for the calculations are

$$E_{g, \text{bulk}} = 1.87 \text{ eV} \quad (\text{bulk bandgap, from } \textit{Thin Solid Films}, \mathbf{515}, 6272 \text{ (2007)})$$

$$V_0 = \frac{5.00 - 1.87}{2} = 1.565 \text{ eV} \quad (\text{potential gap})$$

$$m_e = 0.12 \quad (\text{electron mass, from } \textit{Mater. Sci. Semicond}, \mathbf{40}, 446 \text{ (2015)})$$

$$m_h = 0.21 \quad (\text{hole mass, from } \textit{Mater. Sci. Semicond}, \mathbf{40}, 446 \text{ (2015)})$$

$$\epsilon = 6.7 \quad (\text{relative permittivity, from } \textit{Phys. Status Solidi B}, \mathbf{191}, 115 \text{ (1995)})$$

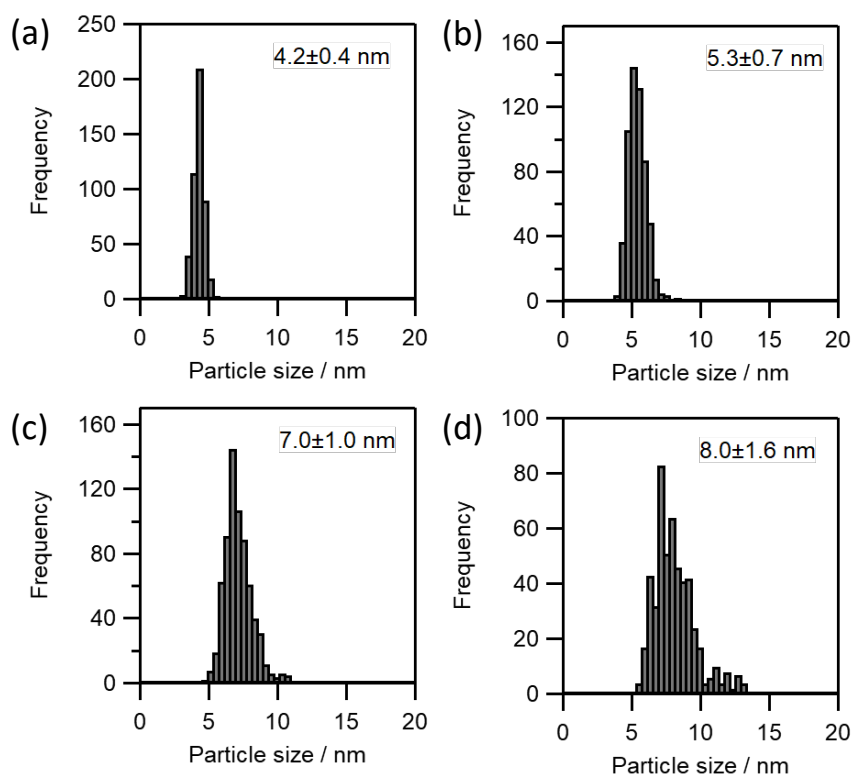


Figure S1. Size distribution histograms for (a) AgInS₂ (AIS) core, (b) AIS/indium sulfide (In-S) core/shell, and AIS/silver indium gallium sulfide (Ag-In-Ga-S)/gallium sulfide (Ga-S) core/graded shell QDs (c) before and (d) after GaCl₃ treatment.

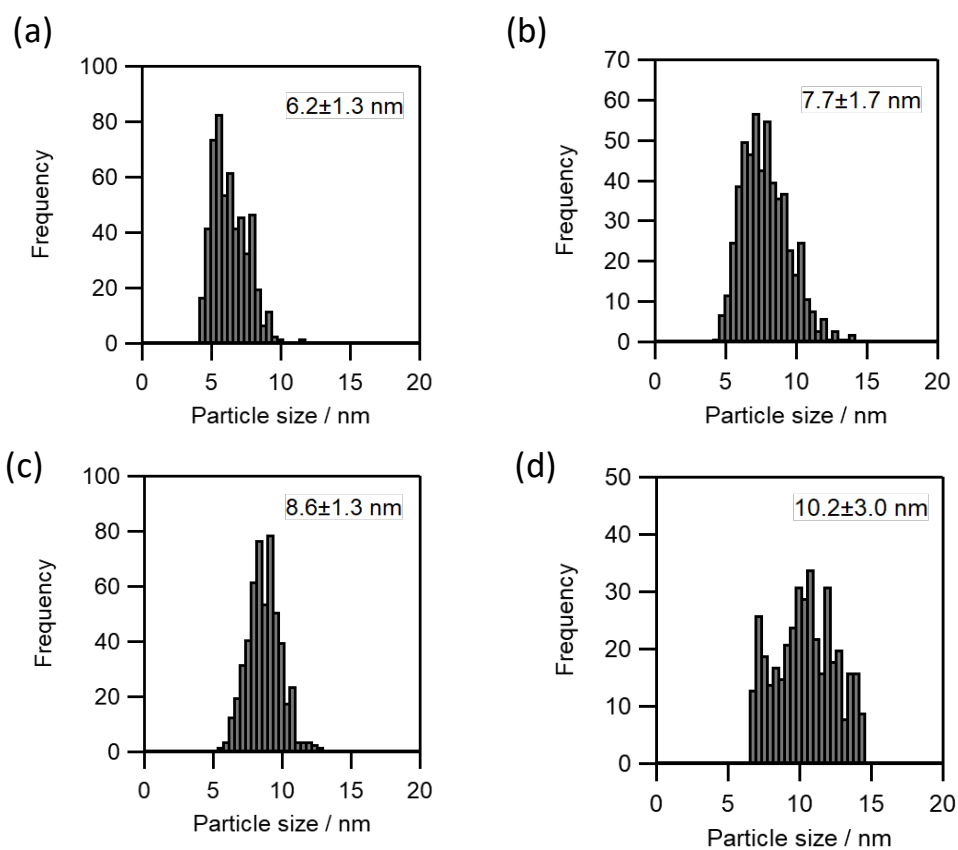


Figure S2. Size distribution histograms for (a, b) AIS/In-S core/shell and (c, d) AIS/Ag-In-Ga-S/Ga-S core/graded shell QDs. Growth temperatures for the In-S shells are (a, c) 200 °C and (b, d) 220 °C.

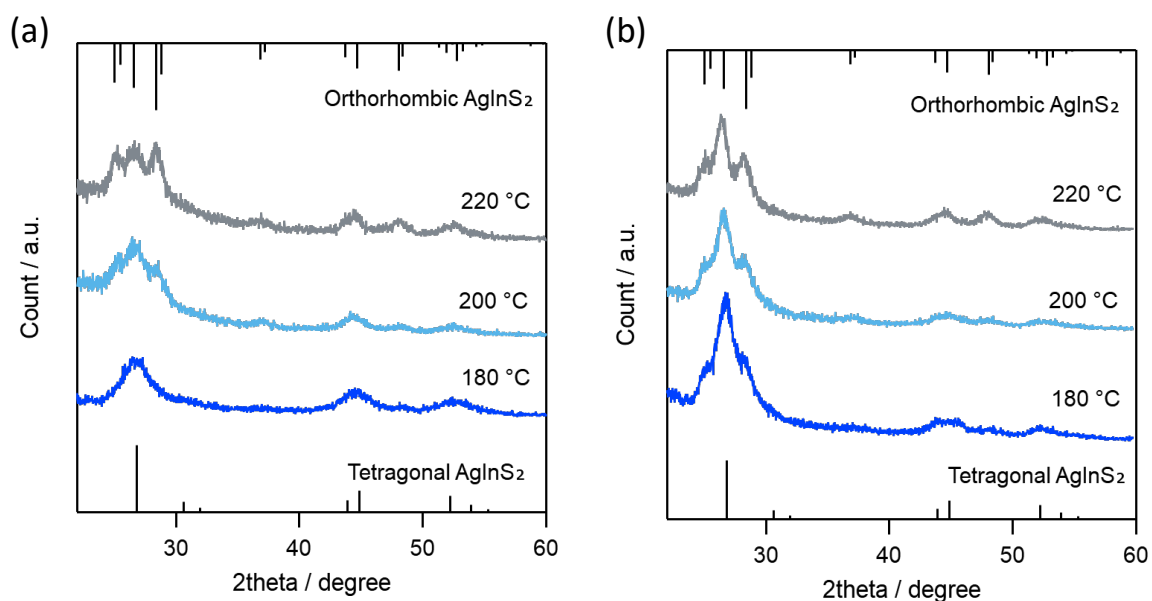


Figure S3. XRD patterns for (a) AIS/In-S core/shell and (b) AIS/Ag-In-Ga-S/Ga-S core/graded shell QDs. The growth temperatures for the In-S shell in each figure are 180°C, 200°C, and 220°C. Reference bars at the top and bottom of the graph correspond to orthorhombic (ICDD 075-6150) and tetragonal AgInS₂ (ICDD 077-6632) phases, respectively.

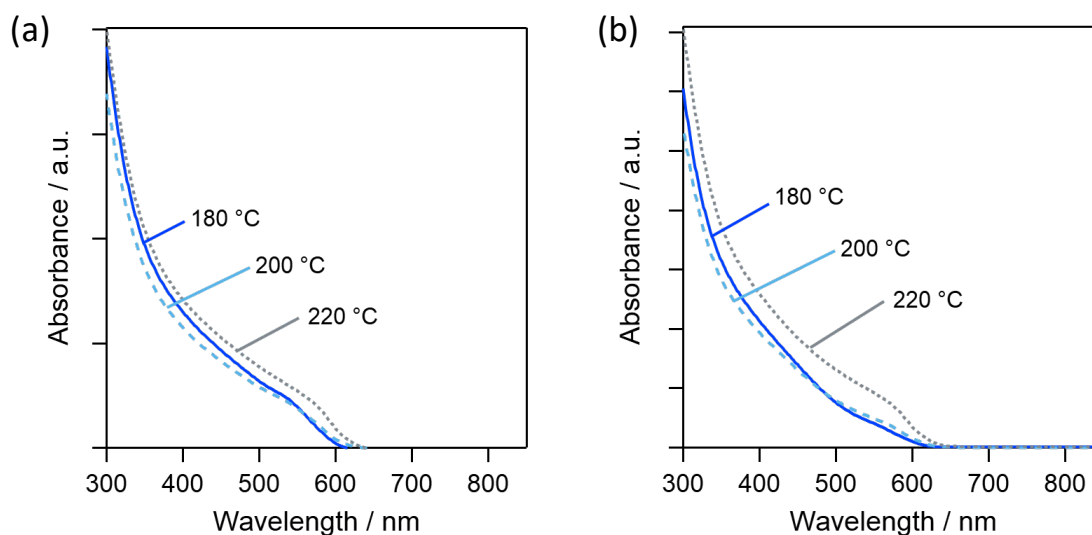


Figure S4. Absorption spectra for (a) AIS/In-S core/shell and (b) AIS/Ag-In-Ga-S/Ga-S core/graded shell at In-S growth temperatures of In-S; 180, 200, and 220 °C



Figure S5. Photograph of AIS/Ag–In–Ga–S/Ga–S core/graded shell QDs under 365-nm UV irradiation, synthesized at In–S growth temperatures of 180 °C (left), 200 °C (middle), and 220 °C (right).

Table S1. PL characteristics of QDs across three synthesis stages, with alteration in reaction temperatures during the In-S coating process.

Sample	In-S growth temperature	PL ^a peak	FWHM ^b (eV)	PL QY ^c (band-edge portion)
AIS core		788 nm (1.57 eV)	0.37	76
AIS/In-S	180 °C	593 nm (2.09 eV) 750 nm (1.65 eV)	– –	23 (1)
AIS/Ag-In-Ga-S/Ga-S (Before GaCl ₃ treatment)		587 nm (2.11 eV)	–	12 (3)
(After GaCl ₃ treatment)		602 nm (2.06 eV)	0.11	48 (32)
AIS/In-S	200 °C	597 nm (2.08 eV) 774 nm (1.60 eV)	– –	17 (1)
AIS/Ag-In-Ga-S/Ga-S (After GaCl ₃ treatment)		612 nm (2.03 eV)	0.12	24 (11)
AIS/In-S	220 °C	614 nm (2.02 eV) 819 nm (1.51 eV)	– –	11 (1)
AIS/Ag-In-Ga-S/Ga-S (After GaCl ₃ treatment)		622 nm (1.99 eV)	0.13	14 (5)

^a Photoluminescence, ^b full-width at half maximum, ^c quantum yield

Table S2. Elemental composition of AIS/In-S core and AIS/Ag-In-Ga-S/Ga-S core/graded shell QDs synthesized with different In-S growth temperatures.

Sample	In-S growth temperature	Composition ratios (Ag = 1.00)			
		Ag	In	S	Ga
AIS/In-S	200 °C	1.00	1.72	3.20	—
AIS/Ag-In-Ga-S/Ga-S ^a		1.00	0.75	2.18	0.35
AIS/In-S	220 °C	1.00	1.76	3.30	—
AIS/Ag-In-Ga-S/Ga-S ^a		1.00	0.71	2.45	0.70

^a After GaCl₃ treatment

Table S3. PL decay components of AIS/In-S core/shell, and AIS/Ag-In-Ga-S/Ga-S core/graded shell QDs synthesized with different In-S growth temperatures.

Sample	In-S growth temp.								
		τ_1/ns	A_1	τ_2/ns	A_2	τ_3/ns	A_3	χ^2	τ_{avg}^b
AIS/In-S	200 °C	3.11	0.703	25.4	0.266	196	0.031	1.02	91
AIS/Ag-In-Ga-S/Ga-S ^a		31.6	0.474	187	0.425	872	0.101	1.07	504
AIS/In-S	220 °C	3.66	0.755	32.4	0.215	234	0.029	1.17	109
AIS/Ag-In-Ga-S/Ga-S ^a		50.7	0.507	287	0.390	1530	0.103	0.92	932

^a After GaCl₃ treatment, ^b Intensity average calculated by $\sum_i A_i \tau_i^2 / \sum_i A_i \tau_i$